

Experimental and Mechanistic Modeling of Fast Pyrolysis of Neat Glucose-Based Carbohydrates. 1. Experiments and Development of a Detailed Mechanistic Model

Xiaowei Zhou,[†] Michael W. Nolte,[‡] Heather B. Mayes,[†] Brent H. Shanks,^{*,‡,§} and Linda J. Broadbelt^{*,†}

[†]Department of Chemical and Biological Engineering, Northwestern University, 2145 Sheridan Road, Evanston, Illinois 60208 United States

[‡]Department of Chemical and Biological Engineering, Iowa State University, 2119 Sweeney Hall, Ames, Iowa 50011, United States

[§]Center for Biorenewable Chemicals (CBiRC), Iowa State University, 1140 Biorenewables Research Laboratory Building, Ames, Iowa 50011, United States

Supporting Information

ABSTRACT: Fast pyrolysis of lignocellulosic biomass, utilizing moderate temperatures ranging from 400 to 600 °C, produces a primary liquid product (pyrolytic bio-oil), which is potentially compatible with existing petroleum-based infrastructure and can be catalytically upgraded to fuels and chemicals. In this work, experiments were conducted with a micropyrolyzer coupled to a gas chromatography–mass spectrometry/flame ionization detector system to investigate fast pyrolysis of neat cellulose and other glucose-based carbohydrates. A detailed mechanistic model building on our previous work was developed for fast pyrolysis of neat glucose-based carbohydrates by integrating updated findings obtained through experiments and theoretical calculations. The model described the decomposition of cellulosic polymer chains, reactions of intermediates, and formation of a range of low molecular weight compounds at the mechanistic level and specified each elementary reaction step in terms of Arrhenius parameters. The mechanistic model for fast pyrolysis of neat cellulose included 342 reactions of 103 species, which included 96 reactions of 67 species comprising the mechanistic model of neat glucose decomposition.

1. INTRODUCTION

The long-term strategy for powering our planet in a sustainable way and reducing emission of carbon dioxide and other greenhouse gases is to replace fossil fuels with renewable resources.¹ Lignocellulosic biomass, which is a potentially renewable source of carbon, has been increasingly recognized as an alternative to petroleum for the production of drop-in transportation fuels and chemicals.^{2–4} Fast pyrolysis, which produces primarily a liquid product (pyrolytic bio-oil) of ~65–75 wt % of the original feedstock, operates in the absence of oxygen at modest temperatures (400–600 °C). Early stage techno-economic evaluations have suggested that fast pyrolysis of biomass could be 2–3 times cheaper than biomass conversion technologies based on fermentation and gasification.⁵

Pyrolytic bio-oil derived from biomass offers potential advantages in its use as a fuel, such as being a renewable source of energy, having low NO_x and SO_x emissions, and reducing net CO₂ input to the atmosphere.¹ However, challenges with bio-oil include poor quality with high oxygen content (up to 60 wt %) and high water content (10–30 wt %) that make it inferior to conventional hydrocarbon fuels, high acidity causing potential corrosion problems, and its unstable and reactive nature that make it difficult to store.⁴ Therefore, it is important to improve the quality and stability of bio-oil.

Pyrolytic bio-oil is a complex mixture of hundreds of organic compounds. The composition of bio-oil derived from fast pyrolysis, which involves multiphase reactions of competing coupled pathways, can be affected by many factors, such as

feedstock types, reaction conditions (e.g., temperature, residence time), or catalysis by indigenous inorganic materials.⁶ A fundamental understanding of the chemistry and kinetics by which fast pyrolysis takes place is critical to unraveling the effects of process parameters on the composition of bio-oil and to improving the quality of bio-oil and the overall economics of the process.

Tremendous efforts have been made in understanding fast pyrolysis of biomass, with extensive studies being devoted to investigating fast pyrolysis of cellulose because it is the most abundant and least complex among the major components of biomass.^{7–11,39} The kinetic models for fast pyrolysis reported in the literature are mostly lumped models, in which cellulose, intermediates, and products were grouped into major products based on phase, i.e., vapors (bio-oil), gas, char, and active cellulose in some cases.^{12,13} The pyrolysis chemistry, despite involving thousands of elementary reactions and yielding hundreds of volatile species, was described by a limited number of global reaction steps between the lumped components. The most representative lumped model for fast pyrolysis of cellulose is the Broido–Shafizadeh model.¹⁴ Léde,¹⁵ White et al.,¹⁵ and Serbanescu¹⁶ reviewed the kinetic lumped models for cellulose pyrolysis. Generally, those global kinetic schemes are able to explain the mass volatilization rates for cellulose and to capture

Received: June 4, 2014

Revised: July 23, 2014

Accepted: July 24, 2014

Published: July 24, 2014

the overall yields of bio-oil, gas, and char from fast pyrolysis. However, they cannot provide fundamental understanding of the detailed decomposition pathways and resulting chemical speciation. Furthermore, it has been emphasized that the rate parameters in lumped models are empirically determined by thermogravimetric analysis or other measures of overall decomposition over a rather narrow range of operating conditions such as feedstock, heating rate, or sample size. Therefore, these lumped models describe pyrolytic decomposition in a limited way, and new models continue to emerge for varying feedstocks and pyrolysis conditions.^{16,17}

In 2012, Vinu and Broadbelt¹⁸ reported the first mechanistic kinetic model for fast pyrolysis of cellulose. The model was built based on the experimental work of Shanks and co-workers^{19–21} using a micropyrolyzer system, isotopic labeling studies of Paine et al.^{22–25} and Ponder and Richards,^{26–28} and quantum chemical calculations of Mayes and Broadbelt²⁹ and many other researchers.^{30–32} Mechanistic modeling has been demonstrated to be effective in elucidating reaction mechanisms and quantifying competing reaction pathways for complex reaction networks.^{18,33} The previous model described the formation of various pyrolysis products at the mechanistic level and was able to closely match the experimental yields of major components of pyrolytic bio-oil including levoglucosan, 5-HMF, 2-furfural, formic acid, glycolaldehyde (GA), and char over a wide range of operating conditions including different starting materials for fast pyrolysis. However, because of the lack of kinetic parameters for some reactions, several parameters were fitted and a temperature exponent was required to match the experimental data at different temperatures. Moreover, the model predictions of the yields of some products were better than others, such as 5-HMF or GA, over a variety of temperatures, which was attributed to either inaccuracy in kinetic parameters for elementary reactions in the model, a lack of inclusion of relevant pathways, or a combination thereof.

A number of experimental and computational efforts have been put forth to gain a better understanding of fast pyrolysis at the mechanistic level during the past two years. New findings are continually emerging. Shanks and co-workers³⁴ performed a careful analysis on the products of fast pyrolysis of glucose, and 24 pyrolysis compounds including 1,6-anhydro- β -D-glucofuranose (levoglucosan-furanose), methyl glyoxal, formaldehyde, acetaldehyde, cyclic hydroxyl lactone, acetone, and propenal were more accurately identified and quantified as compared to their previous experimental work.¹⁹ Recently, Dauenhauer and co-workers⁶ identified 28 compounds in their thin-film pyrolysis experiments. These experimental findings suggest additional pyrolysis chemistry that should be considered in mechanistic modeling of fast pyrolysis.

Computational chemistry calculations have also emerged recently that further illuminate mechanisms and dominant pathways relevant to fast pyrolysis of glucose-based carbohydrates. Mayes et al.³⁴ performed density functional theory (DFT) calculations in a comprehensive study of the elementary mechanisms for glucose conversion to 5-HMF under pyrolysis conditions together with unimolecular 1,2-dehydration reactions of glucose and conversion to the pyranose and furanose forms of levoglucosan. A detailed mechanistic pathway for the formation of the furanose form of levoglucosan from β -D-glucofuranose with the involvement of open D-glucose was reported in that work and by Seshadri and Westmoreland.³⁵ Furthermore, Mayes et al.³⁴ discovered a new pathway from

glucose to 5-HMF via D-fructose as an intermediate, which is more kinetically favorable compared to the pathways reported in the literature to date for the formation of 5-HMF. They also found that 1,2-dehydration reactions of glucose to several anhydro-glucopyranoses required an activation energy as high as 70 or even 80 kcal·mol⁻¹, indicating that those dehydration reactions are very slow under pyrolysis conditions. Quantum chemical calculations of Mayes et al.³⁴ and Seshadri and Westmoreland³⁵ provide kinetic parameters for the interconversion between β -D-glucopyranose to D-glucose, consistent with previous experimental work, such as that by Paine et al.,^{22–25} which found that glucose isomers with acyclic structures play a significant role during fast pyrolysis.

Assary and Curtiss³⁶ computationally investigated the mechanistic pathways from cellobiose to levoglucosanone, in which dehydration of glucose leading to 3,6-anhydroglucopyranose was also discussed. Vasiliou et al.³⁷ studied the pyrolysis of furfural and benzaldehyde and reported the decarbonylation mechanism and its associated kinetic parameters. Agarwal et al.³⁸ performed ab initio molecular dynamics calculations on cellulose and confirmed that levoglucosan is the kinetically favored product of fast cellulose pyrolysis.

Despite these previous efforts, a full map for the mechanistic decomposition of cellulose to various pyrolysis products is still not available. In this work, experiments and mechanistic modeling were conducted to investigate the reaction mechanism of fast pyrolysis of glucose-based carbohydrates including glucose, cellobiose, maltohexaose, and cellulose. The primary purpose of this paper, the first part of this work, was to develop a unified mechanistic model for fast pyrolysis of cellulose as well as other glucose-based carbohydrates by integrating updated findings obtained through experiments and quantum chemical calculations. A complete experimental kinetic study on fast pyrolysis of cellulose at 400–600 °C and glucose, cellobiose, and maltohexaose at 500 °C was performed. Experimental data were used in the second part of this work (DOI 10.1021/ie502260q) to validate and evaluate the mechanistic model and use it to identify and quantify dominant reaction pathways.

2. EXPERIMENTAL SECTION

2.1. Experimental Materials and Methods. Glucose (certified ACS) was purchased from Fisher Scientific and used as received. Cellobiose (>98%), maltohexaose (>90%), and SigmaCell 50 cellulose were purchased from Sigma-Aldrich and used as received. According to Sigma-Aldrich, SigmaCell 50 has an average particle size of 50 μm and a degree of polymerization of ~1900.

A single-shot micropyrolyzer (Model 2020 iS, Frontier Laboratories, Japan) was used for the pyrolysis experiments. In each experiment, a deactivated stainless steel sample cup was loaded with 200–500 μg of carbohydrate and dropped into a preheated furnace. The tubular furnace provided uniform heating and maintained the pyrolysis temperature of 400–600 °C used in this work. A helium flow rate of 105 mL·min⁻¹ through the system was used to sweep the volatile compounds into a Bruker gas chromatograph (430-GC) through a deactivated needle. Before the cup is dropped into the heated furnace, the loaded cup was purged with helium for 30 s to remove oxygen.

A medium polarity capillary column (ZB-1701, Phenomenex) with a stationary phase consisting of 14% cyanopropyl-phenylsiloxane was used for separation of the volatile products.

The gas chromatography (GC) method consisted of an injection temperature of 300 °C and a split ratio of 100:1. The GC temperature started at 35 °C with a hold of 3 min then increased to 300 °C at a rate of 5 °C·min⁻¹ and was held at 300 °C for 4 min. For product identification, the GC was connected to a mass spectrometry (MS) instrument (Saturn 2000), which used electron ionization with a 10 μA emission current in the *m/z* ranging between 30 and 300. The mass spectra of the peaks were compared with standard spectra of chemical compounds within the National Institute of Standards and Technology library database. The chemical identities were verified by running standards of the matching chemicals in the same GC-MS system and comparing retention times and compound fragmentation with the pyrolysis products.

After product identification, a flame ionization detector (FID) was substituted for the MS for higher-accuracy product quantification. The FID was held at 250 °C with an air flow rate of 300 mL·min⁻¹ and hydrogen flow rate of 30 mL·min⁻¹. The pure compounds used in product identification were also used in calibration of the FID results. For the GA calibration, GA dimer was pyrolyzed at about 300 °C resulting in a single sharp peak in its chromatogram, which was proven to be GA by MS. For dianhydro xylose 2 (DAXP 2) and the other dianhydro xylose 2 (other DAXP 2), both of which have a molecular weight of 114, a calibration curve of a similar compound, 4-hydroxy-5-methyl-3-furanone (molecular weight 114), was used to determine their yields. For other AXP, levoglucosanone, cyclic hydroxyl lactone, 1,4:3,6-dianhydro- α -D-glucopyranose, dianhydro glucopyranose, and levoglucosan-furanose, the calibration curve of levoglucosan was applied as a proxy to estimate the yield. Eight-point straight line calibration curves (with $R^2 \geq 0.95$) were obtained by running duplicate standards at four different concentration levels for the pure compounds relating the peak area in the GC-FID chromatogram to their respective standard concentration (or sample weight). The yield of water was estimated because it is not detectable by FID. The yield was estimated by accounting for the amount of water produced in the course of forming dehydration products (e.g., forming 1 mol of levoglucosan also formed 1 mol of water). The water produced from the char-forming reactions was estimated by assuming the char to be 100% carbon. For cellulose, only the char yield was used to estimate water yield, as anhydrosugar formation would cleave the glycosidic bond rather than produce water. Also, the consumption of water in other reactions is not included in the estimation.

For CO and CO₂ quantification, the vent line of the GC was connected to a De-Jaye gas analyzer equipped with an infrared detector. The concentrations of CO and CO₂ were recorded every second. Thus, the yields of CO and CO₂ could be calculated by summing the amount of gas generated over time using the known overall gas flow rate. The char yield was obtained by weighing the sample cup before and after pyrolysis using a Mettler Toledo microbalance with a sensitivity of $\pm 1 \mu\text{g}$.

2.2. Experimental Results. **2.2.1. Fast Pyrolysis of Neat Cellulose at Different Temperatures.** It has been reported that the product distribution of fast pyrolysis of cellulose can be altered significantly by the presence of mineral contaminants such as NaCl and CaCl₂.²⁰ In this work, all the carbohydrate samples contained mineral impurities below threshold level. The effects of transport limitations were eliminated by using samples with particle sizes smaller than 50 μm . Moreover, we have experimental evidence that our system is kinetically

limited. There is no evident change in the molecular structure of individual linear chains of cellulose caused by softening or liquefaction during fast pyrolysis. In addition, we have found no significant differences in the product distributions from fast pyrolysis of cellulose with different crystallinities, degree of polymerization, or feedstock source. Table 1 lists the quantified

Table 1. Yields (in Weight Percent) of the Chemical Species Arising from Fast Pyrolysis of Cellulose at Temperatures Ranging from 400 to 600 °C

compound	400 °C	450 °C	500 °C	550 °C	600 °C
formaldehyde	0.12	0.37	0.40	0.57	0.93
acetaldehyde	0.09	0.34	0.68	1.07	1.78
methanol	0.00	0.07	0.14	0.11	0.09
furan	0.06	0.06	0.08	0.10	0.13
propenal	0.02	0.16	0.30	0.56	1.01
acetone	0.02	0.03	0.06	0.09	0.13
methyl glyoxal	0.49	0.69	1.13	1.15	1.26
2-methyl furan	0.04	0.03	0.05	0.10	0.18
vinyl acetate	0.01	0.03	0.11	0.20	0.33
glycolaldehyde	4.81	6.30	7.88	6.56	6.05
acetic acid	0.01	0.05	0.10	0.11	0.11
acetol	0.14	0.35	0.38	0.54	0.46
MW 86	0.02	0.04	0.26	0.14	0.05
furfural	0.32	0.35	0.33	0.41	0.32
2-furanmethanol	0.06	0.05	0.07	0.05	0.02
3-furanmethanol	0.01	0.02	0.04	0.03	0.04
MW 102	0.07	0.08	0.08	0.08	0.08
2-hydroxy-cyclopent-2-en-1-one	0.06	0.10	0.15	0.15	0.24
5-methyl furfural	0.02	0.02	0.05	0.03	0.05
2(5H)-furanone	0.07	0.10	0.13	0.11	0.10
MW 114 DAXP 2	0.36	0.42	0.47	0.57	0.42
methyl cyclopentenolone	0.04	0.04	0.07	0.03	0.06
other DAXP 2	0.12	0.17	0.18	0.15	0.15
levoglucosanone	0.37	0.27	0.25	0.38	0.38
cyclic hydroxyl lactone	0.20	0.49	0.36	0.30	0.13
1,4,3,6-dianhydro- α -D-glucopyranose	0.76	1.17	1.72	2.24	2.53
5-hydroxy methyl furfural	1.28	1.32	0.92	1.10	1.06
dianhydro glucopyranose	6.72	6.19	4.90	4.01	2.67
other AXP	0.77	0.47	0.45	0.32	0.45
levoglucosan-pyranose	69.50	60.71	54.50	53.34	50.85
levoglucosan-furanose	3.08	2.98	2.31	2.19	2.07
CO	1.62	1.61	1.84	2.09	2.60
CO ₂	4.64	5.06	3.57	2.99	3.91
char	3.09	4.33	4.57	3.98	2.77
H ₂ O	4.64	6.50	6.86	5.97	4.16

speciation results for fast pyrolysis of cellulose at five temperatures ranging from 400 to 600 °C. All pyrolysis experiments were conducted with at least three replications. Standard deviations of the product yields for the triplicate runs of cellulose pyrolysis are given in Table S1 in the Supporting Information. This experimental data will be used to validate the mechanistic model in the second part of this study (DOI 10.1021/ie502260q). A total of 32 pyrolysis products including H₂O were identified in the experiments (please note that we no longer use primary products or secondary products to label the pyrolysis products because pyrolysis reactions in the melt phase involve complex primary reactions of the feedstock and secondary reactions of the primary products and intermediates). As shown in Table 1, levoglucosan-pyranose, levogluco-

san-furanose, GA, 5-HMF, methyl glyoxal, char, CO₂, CO, and H₂O were the major pyrolysis products with a yield of more than 1 wt %. The total yield of these products summed to 90 wt %. Levoglucosan-pyranose was the dominant product of fast pyrolysis of cellulose, and its yield decreased monotonically from 69.5 to 50.85 wt % as pyrolysis temperature increased from 400 to 600 °C. Experiments on fast pyrolysis of neat levoglucosan at different temperatures showed that there was no degradation occurring during fast pyrolysis, which was also consistent with the experimental work of Patwardhan et al.¹⁹ The yields of small compounds such as formaldehyde, acetaldehyde, propenal, acetone, and CO increased as the temperature increased, indicating that the formation of these products involved reactions with energy barriers higher than those for formation of levoglucosan-pyranose. GA, 5-HMF, cyclic hydroxyl lactone, CO₂, and char increased in yield then decreased with increasing pyrolysis temperature. This result indicated that the formation of these compounds was competing with reactions with a higher activation energy, the compounds underwent further degradation at high temperatures, or a combination thereof.

2.2.2. Fast Pyrolysis of Neat Glucose, Celllobiose, and Maltohexaose at 500 °C. Table 2 lists the final yields of various products from fast pyrolysis of glucose, cellobiose, maltohexaose, and cellulose at 500 °C. The data for cellulose is the same as that reported in Table 1 at 500 °C but is repeated for ease of comparison. Standard deviations of the product yields for the triplicate runs of fast pyrolysis of glucose, cellobiose, and maltohexaose are given in Table S2 in the Supporting Information.

As shown in Table 2, levoglucosan-pyranose, levoglucosan-furanose, GA, 5-HMF, char, CO₂, CO, and H₂O remain the major pyrolysis products for fast pyrolysis of monosaccharide glucose, disaccharide cellobiose, and oligosaccharide maltohexaose at 500 °C. Another feature is that the yields of some of the pyrolysis products were a strong function of the chain length of the carbohydrate. Specifically, there was a sharp decrease in the yield of levoglucosan-pyranose and a significant increase in the total yield of other low molecular weight (LMW) products (including H₂O and gaseous fraction) from cellulose to glucose. The yields of many other low molecular weight products (LMWPs) such as 5-HMF, levoglucosan-furanose, CO₂, char, levoglucosenone, furfural, acetone, and acetol were much higher from glucose pyrolysis than from cellulose pyrolysis, which indicated that the formation of these LMWPs may require the involvement of glucose or its derivative as an intermediate during fast pyrolysis.

3. MECHANISTIC MODELING

3.1. Reaction Mechanism. The first step in building a mechanistic model for fast pyrolysis of glucose-based carbohydrates is to identify all the possible reaction steps for the formation of the experimentally observed products. A concerted mechanism has been demonstrated to be more kinetically favorable than radical and ionic mechanisms and offers better alignment with experimental findings;²⁹ thus, our model is based on concerted reactions. In this model, concerted reactions of fast pyrolysis are classified into two general categories: (i) decomposition of the cellulose chains and (ii) reactions of the LMW species that are formed from cellulose. Because it is not clear from experimental data alone if all the pyrolysis products are exclusively formed from the cellulose chain or through intermediate species, we have included both

Table 2. Yields (in Weight Percent) of the Chemical Species Arising from Fast Pyrolysis of Glucose-Based Carbohydrates at 500 °C

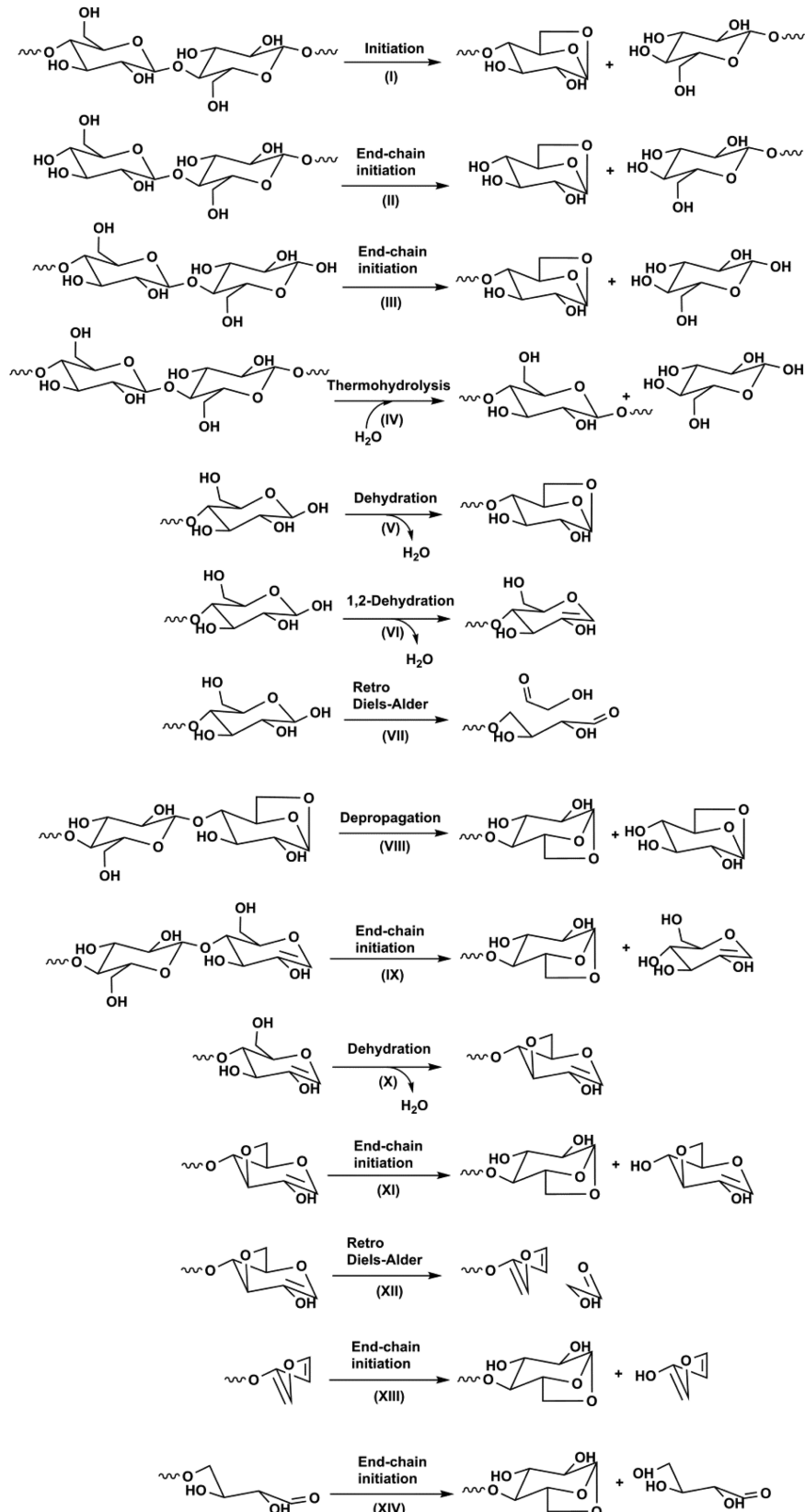
compound	glucose	cellobiose	maltohexaose	cellulose
formaldehyde	0.41	0.51	0.36	0.40
acetaldehyde	0.61	0.47	0.39	0.68
methanol	0.32	0.18	0.06	0.14
furan	0.15	0.22	0.06	0.08
propenal	0.18	0.21	0.14	0.30
acetone	0.11	0.06	0.04	0.06
methyl glyoxal	1.50	0.89	1.17	1.13
2-methyl furan	0.12	0.07	0.04	0.05
vinyl acetate	0.25	0.26	0.26	0.11
glycolaldehyde	5.21	7.14	8.46	7.88
acetic acid	0.32	0.14	0.14	0.10
acetol	0.59	0.30	0.44	0.38
dihydroxyacetone	0.11	0.07	0.13	0.05
MW 86	0.40	0.37	0.20	0.26
furfural	0.96	0.82	0.33	0.33
2-furanmethanol	0.09	0.05	0.22	0.07
3-furanmethanol	0.12	0.03	0.03	0.04
MW 102	0.12	0.12	0.03	0.08
2-hydroxy-cyclopent-2-en-1-one	0.35	0.27	0.25	0.15
5-methyl furfural	0.13	0.08	0.06	0.05
2(SH)-furanone	0.08	0.10	0.10	0.13
MW 114 DAXP 2	0.11	0.07	0.13	0.47
methyl cyclopentenolone	0.10	0.08	0.09	0.07
other DAXP 2	0.14	0.10	0.14	0.18
levoglucosenone	0.61	0.38	0.30	0.25
cyclic hydroxyl lactone	0.77	1.58	0.85	0.36
1,4,3,6-dianhydro- α -D-glucopyranose	0.38	0.97	0.63	1.72
5-hydroxy methyl furfural	4.93	3.35	1.75	0.92
dianhydro glucopyranose	0.07	0.96	1.84	4.90
other AXP	0.24	0.27	0.08	0.45
levoglucosan	8.10	27.23	33.11	54.50
levoglucosan-furanose	3.96	2.14	0.51	2.31
CO	1.20	1.11	1.23	1.84
CO ₂	7.56	6.10	6.11	3.57
char	9.34	5.72	5.51	4.57
H ₂ O	18.96	14.88	14.00	6.86

possibilities for product formation. The concerted pathways are described in the following sections.

3.1.1. Reactions of Cellulose Chains. The reactions of cellulose chains are further classified into two types in terms of end-groups and mid-groups. Scheme 1 depicts the concerted reactions of cellulose chains involving end-groups. The model includes initiation of cellulose chains (reaction I) yielding levoglucosan-end (LVG-end) chains and nonreducing-end (NR-end) chains, formation of levoglucosan via end-chain initiation (reaction II) and depropagation (reaction VIII), and formation of glucose via end-chain initiation (reaction III) and thermohydrolysis (reaction IV), which have been reported in our previous model.¹⁸

Apart from the above reactions that form glucose and levoglucosan, additional reactions yielding other LMWPs were incorporated into the model. As shown in Scheme 1, dehydration (reaction V), 1,2-dehydration (reaction VI), and retro-Diels–Alder (reactions VII and XII) can occur to the far right glucose unit of the cellulose chain (direction is arbitrarily defined but used for clarity in discussion), affording chains with

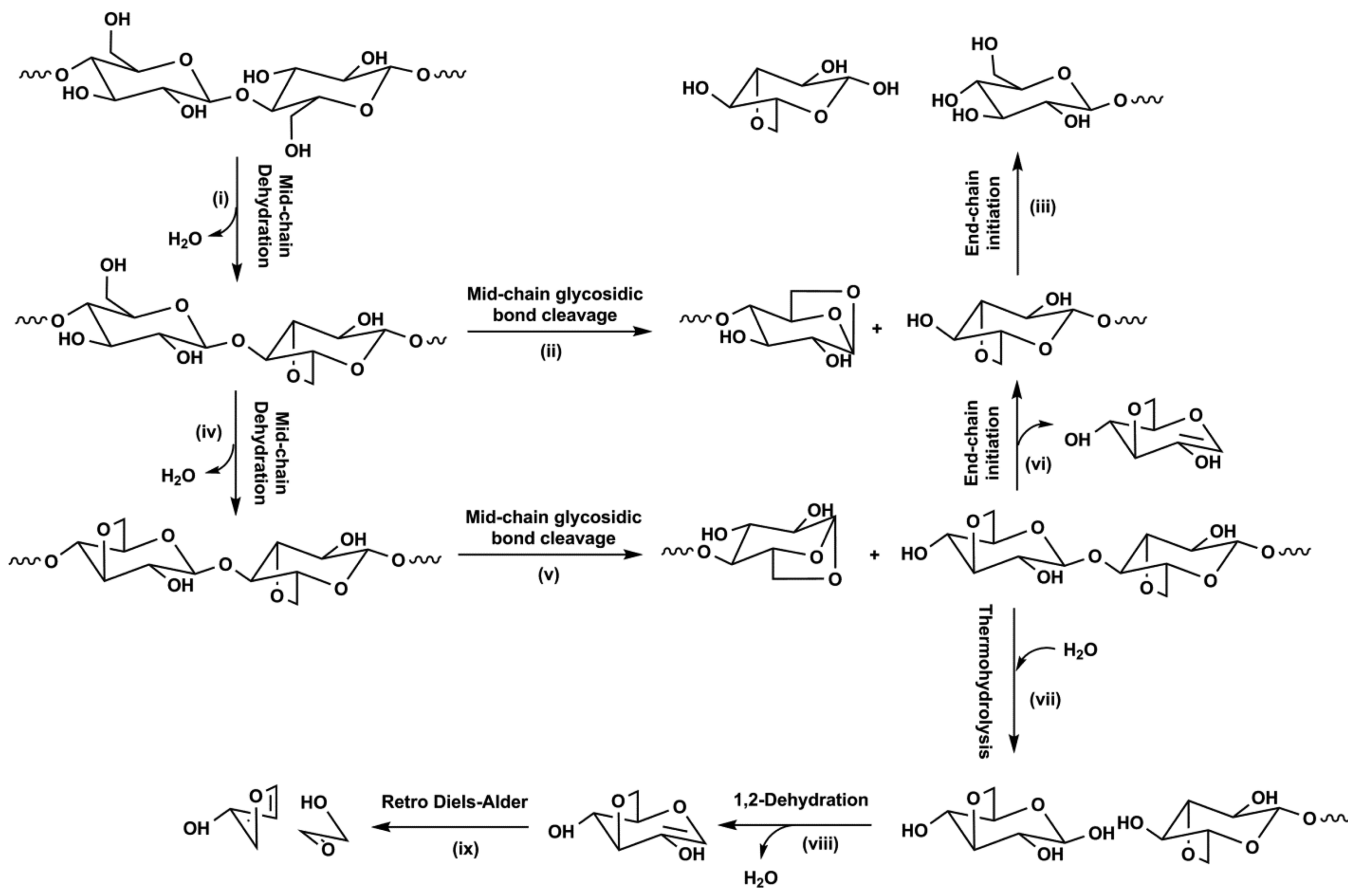
Scheme 1. Decomposition Mechanisms of Cellulose/Maltohexaose Chains Involving End-Groups



a LVG-end, 1,2-anhydro-glucopyranose-end, and erythrose-end, respectively. 1,2-Anhydro-glucopyranose-end chains can undergo a further dehydration reaction and form 1,2:3,6-dianhydroglucopyranose-end chains, from which GA and a chain with a

furanol-end can be formed via a retro-Diels–Alder reaction. All the chains with LMWP-ends undergo end-chain initiation and yield a LVG-end chain and a molecule of corresponding LMWPs (reactions IX, XI, XIII, and XIV).

Scheme 2. Decomposition Mechanisms of Cellulose/Maltohexaose Chains Involving Mid-Groups



As shown in Scheme 2, another type of reaction that occurs for cellulose and its derived chains is midchain dehydration. A large amount of water being produced from cellulose pyrolysis was observed in the experiments, which indicates that dehydration occurs to cellulose chains during pyrolysis. In our first model, midchain-1,2-dehydration followed by glycosidic bond cleavage (GBC) and retro-Diels–Alder were included to afford GA from cellulose. However, Mayes et al.³⁴ recently discovered that the activation energy required for 1,2-dehydration of glucose affording 2,3-anhydro-glucopyranose is as high as $72 \text{ kcal}\cdot\text{mol}^{-1}$, indicating that this dehydration reaction is not competitive under fast pyrolysis conditions. However, dehydration of glucose by losing water with the involvement of HO₆ and the hydroxyl connected with C1–C4 (molecular structure and atom numbering scheme of glucose are shown in Figure S1 in the Supporting Information) is more facile than the 1,2-dehydration of glucose. For example, the activation energy required for the 1,2-dehydration of glucose involving the loss of the OH group at C1 and H1 is $62 \text{ kcal}\cdot\text{mol}^{-1}$, while a much lower E_a of $48 \text{ kcal}\cdot\text{mol}^{-1}$ is required for the dehydration to lose the OH group at C1 and HO₆ to form a molecule of water. They revealed that the likelihood of forming a molecule of water by losing a hydroxyl group connected with C1–C4 and HO₆ from glucose via dehydration follows the order C1 < C3 < C2 < C4. The hydroxyl group at glucose C1 no longer exists in the mid-groups of cellulose because cellulose is a homopolymer of glucose residues connected by β -(1–4) glycosidic linkages (C1–O₁–C4). Therefore, dehydration occurring within cellulose chains favors the formation of water by losing HO₆ and other hydroxyl

groups, most likely the OH group at C3. Quantum chemical calculations of Assary and Curtiss³⁶ reported that the predominant yield of 1,6-anhydroglucopyranose from cellulose pyrolysis is attributed to its formation through the initial ether bond cleavage, while the formation of 3,6-anhydroglucopyranose during the pyrolysis can be explained by the dehydration of glucose, which is endothermic at room temperature. Seshadri and Westmoreland³⁵ stated that levoglucosan and anhydro-glucose-pyranose were principal bicyclic products from glucose and cellulose and that they were formed by dehydration reactions. Furthermore, 1,4:3,6-dianhydro-glucopyranose has been experimentally identified and quantified from the volatile products of fast pyrolysis of cellulose.^{40,41} All these findings support the midchain dehydration of cellulose (reaction i), as shown in Scheme 2. Cellulose can undergo midchain dehydration to form a 3,6-anhydro-glucopyranose-midchain. Because cellulose contains hundreds of β -(1–4) linked D-glucose units, the possibility that midchain dehydration occurred to give a dehydrated mid-group of cellulose is also included in the model, as depicted by reaction iv. The dehydrated mid-groups subsequently undergo concerted midchain GBC similar to initiation and yield a LVG-end chain and a 3,6-anhydro-glucopyranose-end chain (reactions ii and v). Then, 1,2:3,6-dianhydro-glucopyranose is released via end-chain initiation of 3,6-anhydro-glucopyranose-end-chains (reactions iii and vi). Assary and Curtiss³⁶ modeled the breaking of the ether bond of cellobiose in the gas phase through hydrogen transfer from the C2 atom of the glucose subunit to the ether oxygen, which produced 1,2-dehydroglucopyranose and β -D-glucopyranose. Thus, reactions iii and vi

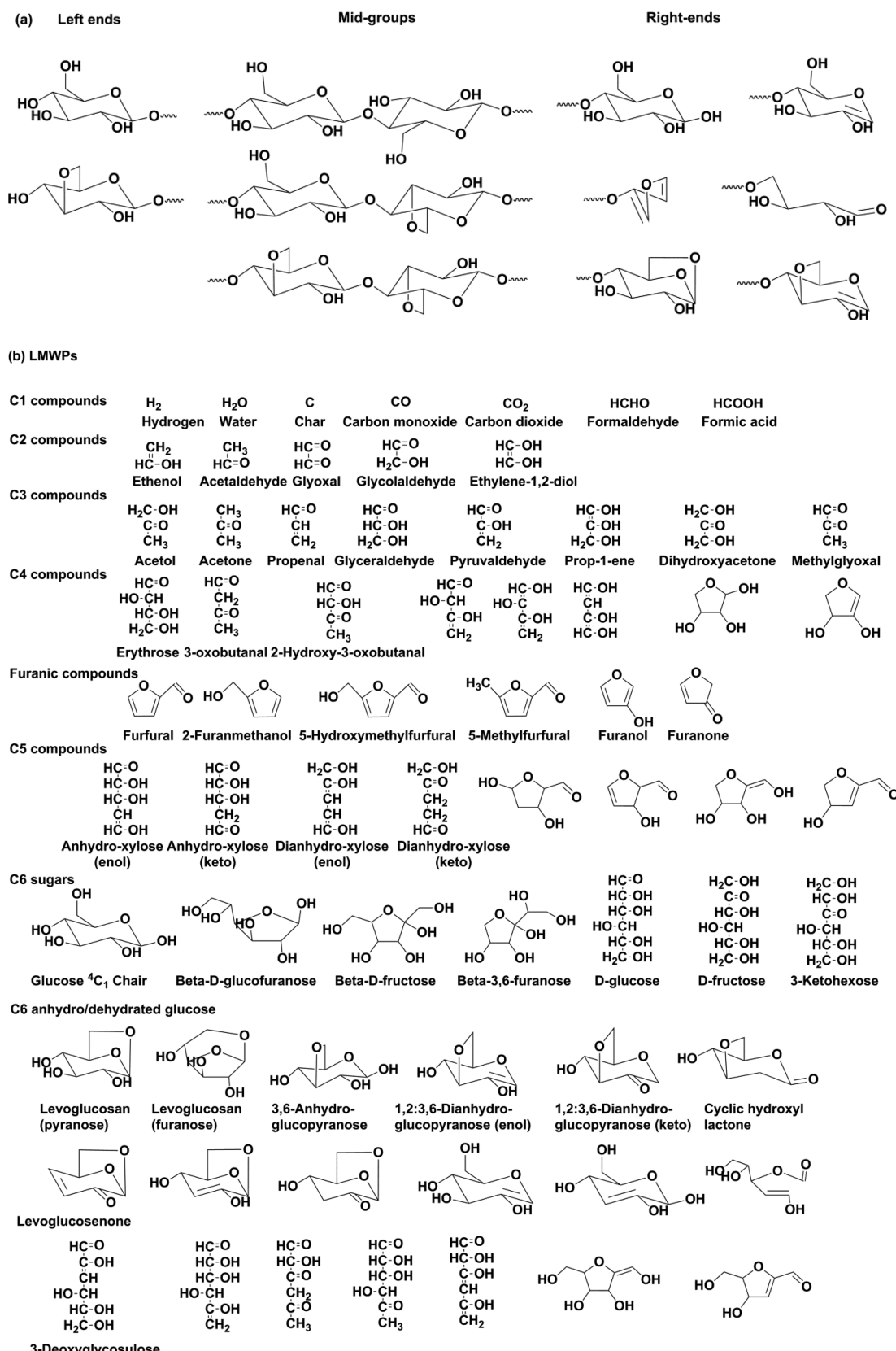
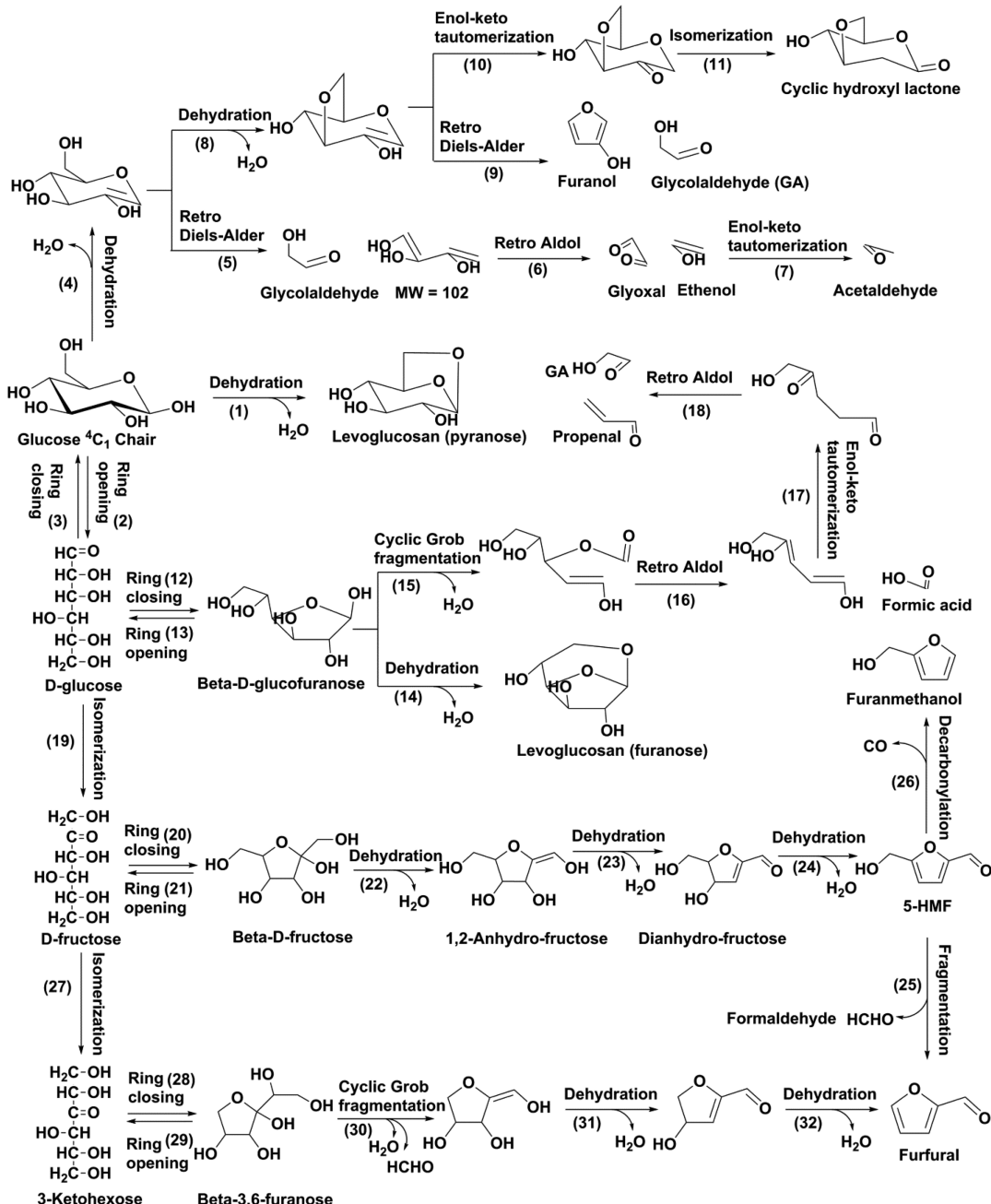


Figure 1. (a) Identity of cellulosic chains based on end-groups and mid-groups. (b) List of 67 LMW species tracked in the fast pyrolysis model.

are certainly viable because the midchain dehydration results in the connection of O6 with C3, and therefore the plausible product from the breaking of the ether bond, is 1,2:3,6-dianhydro-glucopyranose. Moreover, experiments observed

significant amounts of unidentified dianhydro-glucopyranose. Reaction vii represents thermohydrolysis, by which 3,6-anhydro-glucopyranose is released from the chains. Water

Scheme 3. Reaction Mechanism of β -D-Glucopyranose to Form a Variety of C1–C6 Compounds during Fast Pyrolysis

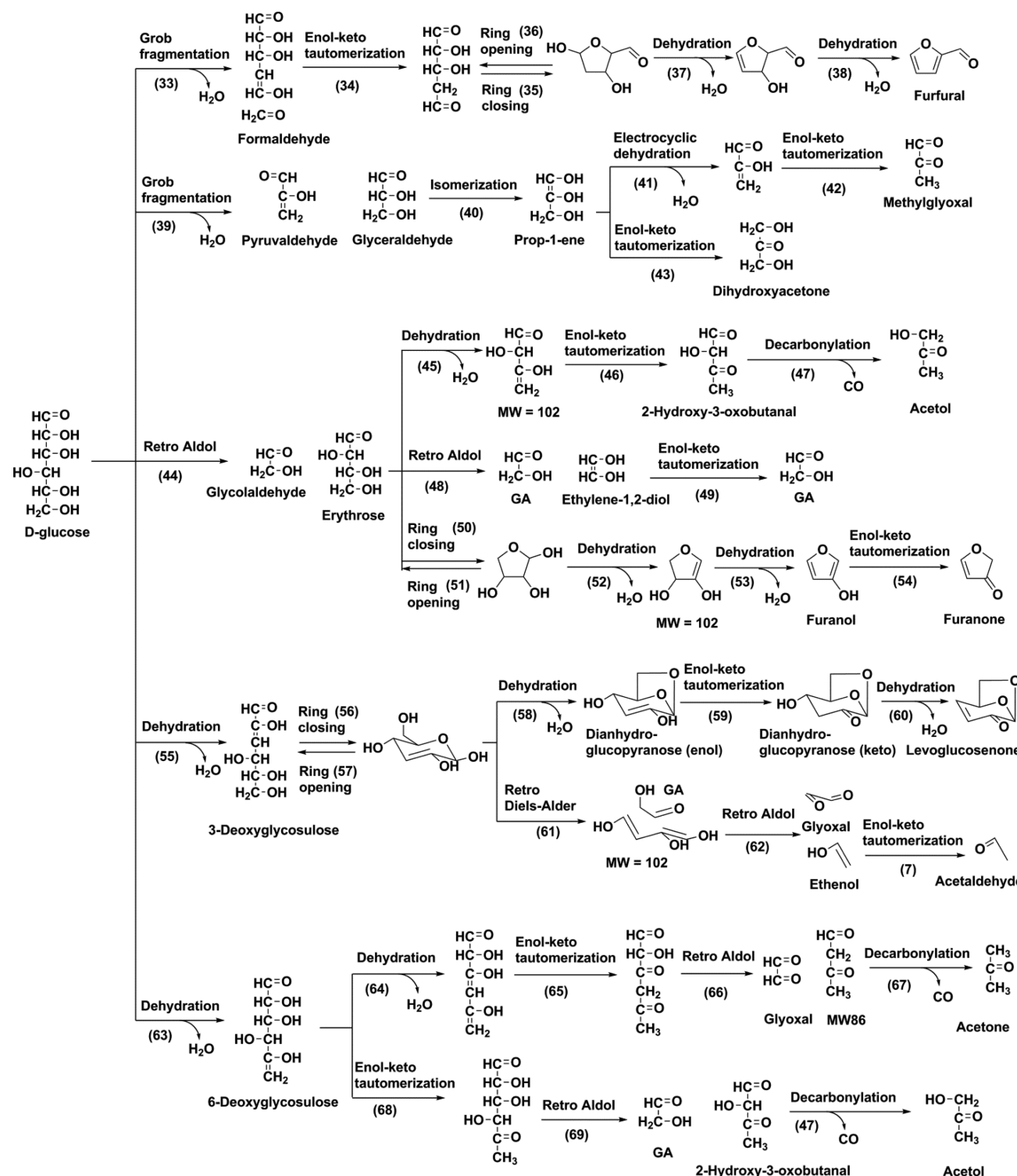
partaking in the thermohydrolysis reaction is mainly produced from cellulose dehydration reactions.

Retro-Diels–Alder has been reported to be important for the formation of GA from cellulose pyrolysis.^{26,42} Shen et al.⁴³ experimentally investigated cellulose pyrolysis and proposed the possible routes for the formation of the main products from the direct conversion of cellulose, in which GA was formed from C1–C2 of cellulose via a retro-Diels–Alder reaction. Carstensen and Dean⁴² utilized quantum chemistry to explore typical retro-Diels–Alder reactions in biomass conversion, and their results indicated that the time scale of reaction ii in glucose was comparable to the typical reaction time scales of 1–5 s in fast pyrolysis. Slamet and Wege⁴⁴ and Shen et al.³² also reported degradation of glucose via a retro-Diels–Alder reaction during pyrolysis, suggesting that this reaction is feasible

in fast pyrolysis. Therefore, we have included this reaction in the model. Reaction VII depicts the formation of GA from C5–C6 of cellulose, and reactions XII and ix represent the retro-Diels–Alder reaction, by which GA is formed from C1–C2 of cellulose.

3.1.2. Reaction Network of Glucose Intermediate and LMWP_s. This mechanistic reaction network begins with the assumption that glucose serves as an intermediate in the formation of smaller compounds, which has been reported in the literature.^{18,28,45–47} The degradation of β -D-glucopyranose in our first mechanistic model proceeded through 1,2-dehydration reactions to give anhydro-glucopyranose and ring-opening to form D-glucose.¹⁸ However, recent quantum chemical calculations of Mayes et al.³⁴ revealed that several 1,2-dehydration reactions of β -D-glucopyranose to anhydro-

Scheme 4. Continued Mechanism of the Formation of C1–C6 Compounds



glucopyranose, which led to the formation of important pyrolysis products such as 5-HMF, GA, furfural, acetol, acetaldehyde, and formaldehyde in our first mechanistic model for cellulose pyrolysis,¹⁸ are high in energy barriers and thus are slow.

Here, we propose mechanistic steps that incorporate these new findings and including additional new pathways that lead to the formation of pyrolysis products such as 1,6-anhydro- β -D-glucofuranose, levoglucosenone, methyl glyoxal, dihydroxyace-

tone, propenal, and acetone, all of which were not included in our previous model.

Figure 1 lists the 67 LMWPs tracked in the model as compared to the 40 LMWPs in our previous model. Schemes 3–5 depict the mechanistic reactions starting from β -D-glucopyranose in the chair conformation (4C_1). The detailed reaction pathways are outlined below.

3.1.2.1. Reaction of β -D-glucose. Besides the formation of levoglucosan directly from the chain decomposition, a one-step

dehydration of glucose (reaction 1) that has been widely reported is included in the model. There is long debate on whether levoglucosan undergoes secondary reactions during fast pyrolysis. Levoglucosan has a melting point of 182–184 °C and a boiling point of 384 °C. At a typical pyrolysis temperature of 500 °C, levoglucosan would be volatilized effectively before its secondary decomposition takes place as long as its gas-phase partial pressure is sufficiently low. Furthermore, our experiments showed that no degradation was observed in fast pyrolysis of neat levoglucosan using the micropyrolyzer system. Therefore, this model includes the formation of levoglucosan from glucose via dehydration and covers no secondary reactions of levoglucosan.

Reaction 4 represents 1,2-dehydration of β -D-glucopyranose to 1,2-anhydro-glucopyranose, which is the only 1,2-dehydration of β -D-glucopyranose included in the model. This is the most feasible because it requires the lowest energy barrier, according to DFT calculations of Mayes et al.,³⁴ and all the frequency factors are assumed to be the same according to the reaction family approach.

As depicted in Scheme 3, the model includes various transformations between β -D-glucopyranose and its cyclic and acyclic isomers via ring-opening/ring-closing and isomerization. Quantum chemical calculations revealed that the interconversion of β -D-glucopyranose and acyclic D-glucose is feasible via ring-opening and ring-closing reactions and that transformations of β -D-glucopyranose to its other isomers occur through acyclic D-glucose. The acyclic structure is a key intermediate to the formation of glucose isomers such as β -D-glucofuranose, fructose, and 3-ketohexose, and also to the formation of a range of LMW products, which are shown in Scheme 4. Although glucose can also isomerize to α -D-glucose from D-glucose by a unimolecular pathway with a four-center transition state, quantum chemical calculations and experimental efforts of Mayes et al.³⁴ revealed that no significant difference was observed between α - and β -glucose in terms of overall reaction behavior during fast pyrolysis. Dauenhauer and co-workers⁴⁸ also reported that product yields from fast pyrolysis of glucose-based carbohydrates with β -linkages or α -linkages showed no difference. Therefore, the model does not include α -D-glucose and its decomposition reactions. Furthermore, transformations of β -D-glucopyranose to its other isomers such as hexenhexol, α -D-glucofuranose, fructofuranose, and 3,6-furanose are also not included in this model because either these pathways involve very high energy barriers or these isomers play a negligible role in pyrolysis as revealed by ¹³C isotopic labeling studies^{23–25} and quantum chemical calculations.³⁵

3.1.2.2. β -D-Glucofuranose and Pathway to Anhydro- β -D-glucofuranose and Formic Acid. Anhydro- β -D-glucofuranose is a minor product of glucose fast pyrolysis with yields ranging from 2 to 5 wt %. The formation of anhydro- β -D-glucofuranose involves the transformation of β -D-glucopyranose to its cyclic isomer β -D-glucofuranose through D-glucose. Pathway 2-12-14 represents the formation of anhydro- β -D-glucofuranose from β -D-glucopyranose via ring opening, ring closing, and dehydration. This unimolecular path is consistent with DFT calculations of Mayes et al.³⁴ and Seshadri and Westmoreland.³⁵

Once β -D-glucofuranose is formed, it can undergo further decomposition leading to the formation of formic acid according to experimental work of Paine et al.,²³ which indicated half of the formic acid was derived from C1 of the glucose unit. Pathway 15-16 represents the formation of formic

acid from glucose, in which β -D-glucofuranose unravels via cyclic Grob fragmentation to give a molecule of water and a hydroxyallyl ester, which undergoes retro-aldol to form formic acid derived from C1, simultaneously affording a dominant route to acrolein as reported by Paine et al.²⁴

3.1.2.3. D-Fructose and Pathway to 5-HMF. Sanders et al.⁴⁹ observed that the yield of furans was higher in glucose pyrolysis compared to that in cellulose pyrolysis, which suggests that there is a significant isomerization to acyclic forms in glucose pyrolysis. The derivatives of D-fructofuranose such as furfural and 5-HMF are present in the products of pyrolysis of D-glucose and D-fructose, indicating that there is a significant interconversion between D-glucose and D-fructose. ¹³C isotopic labeling studies of Paine et al.²⁵ on pyrolysis of D-glucose and D-fructose demonstrated that D-fructose is engaged in the formation of 5-HMF. Lin et al.⁵⁰ revealed that 5-HMF is more favorable to be formed from D-fructose than from D-glucose. Mayes et al.³⁴ performed a comprehensive comparison of pathways to 5-HMF reported in the literature and carried out pathway screening using quantum chemistry methods. Here, we included the most kinetically favorable pathway that Mayes et al.³⁴ revealed for the formation of 5-HMF, in which D-fructose undergoes a ring-closing reaction followed by three dehydration reactions to give 5-HMF, shown as reactions 2-19-20-22-23-24 in Scheme 3. D-Fructose is an acyclic ketone formed from D-glucose through unimolecular isomerization (reaction 19) involving a six-centered transition state. D-fructose can react similarly to form β -D-fructose with a five-membered ring structure (reaction 20), which involves the carbonyl group at C2 and the group at C5. Then dehydration of β -D-fructose yields a molecule of water and a fructose enol that undergoes 1,2-dehydration and yields an intermediate from which 5-HMF is formed.

3.1.2.4. 3-Ketohexose and Pathway to Furfural. DFT calculations of Seshadri and Westmoreland³⁵ revealed that formation of 3-ketohexose from D-fructose has a lower activation energy of 46.8 kcal·mol⁻¹ as compared to 61.2 kcal·mol⁻¹ from D-glucose via a six-centered transition state with a strained geometry. Paine et al.²³ speculated that 3-ketohexose was involved in the formation of furfural according to the ¹³C isotopic labeling study of pyrolysis of glucose. The pathway 2-19-27-28-30-31-32 represents the formation of furfural from 3-ketohexose. In the present work, two additional pathways to furfural are also included. One is the pathway 33-34-35-37-38 from D-glucose. The other is a one-step fragmentation of 5-HMF (reaction 25), which simultaneously releases a molecule of formaldehyde and furfural. Literature support can be found for this fairly short pathway to rationalize the formation of furfural from 5-HMF.^{25,37}

3.1.2.5. Reactions of Acyclic D-Glucose. Paine et al.²³ revealed that mechanisms involving D-glucose are more important than those involving D-fructose, which plays a more important role than 3-ketohexose during fast pyrolysis. Their isotopic labeling with ¹³C suggested that cyclic Grob fragmentation, retro-aldol, and dehydration were the concerted reactions by which D-glucose was broken down to small molecules during fast pyrolysis. Scheme 4 depicts the formation of various pyrolysis products from intermediate D-glucose.

3.1.2.6. Glycolaldehyde. Experiments found that glycolaldehyde is normally a major product of fast pyrolysis of glucose-based carbohydrates. Isotopic labeling studies indicate that 40% of GA comes from C1–C2, 35% from C3–C4, and 25% from C5–C6.²³ In this model, besides the formation of GA from

chain decomposition (reactions VII, XII, and ix), several routes for the formation of GA via intermediate glucose are also included. Pathways 4-5 and 2-55-56-61 involve dehydration to form anhydroglucopyranose, followed by a retro-Diels–Alder reaction to afford GA. Pathway 4-9 and reaction ix represent the formation of GA from C1–C2 of dianhydro-glucopyranose, which also provide a route for the formation of cyclic hydroxyl lactone.⁵¹ Pathway 2-12-15-16-18 represents GA formed via retro-aldol reaction of a C5 fragment derived from β -D-glucofuranose. This is a minor pathway for GA formation. Pathway 2-44-48-49 yields the formation of three molecules of GA from C1–C2, C3–C4, and C5–C6 fragments. This is a widely reported and well-recognized pathway for the formation of GA from glucose.^{23,26,35} It involves retro-aldol reaction of acyclic D-glucose forming GA and erythrose, followed by retro-aldol reaction of erythrose to form GA and 1,2-ethylene diol and enol-keto tautomerization of 1,2-ethylene diol to GA. Retro aldol reactions are generally competitive under pyrolysis conditions because of the low activation energy of this unimolecular decomposition. Pathway 2-63-68-69 also invokes a final retro-aldol step to release GA with the coformation of 2-hydroxy-3-oxobutanal.

3.1.2.7. 2-Hydroxy-3-oxobutanal and Pathway to Acetol. 2-Hydroxy-3-oxobutanal has been reported as a product from pyrolysis of various types of biomass.^{52,53} As shown in Scheme 4, the model includes two pathways to acetol, both of which involve a final step of decarbonylation of 2-hydroxy-3-oxobutanal to yield carbon monoxide and acetol (reaction 47). The formation of acetol from 2-hydroxy-3-oxobutanal is consistent with the ¹³C-labeling results of Ponder and Richards,²⁸ which also showed that acetol mostly derived from contiguous terminal carbons (C1–C2–C3 or C4–C5–C6), and the acetol methyl groups were from a terminal carbon (C1 or C6).

3.1.2.8. Levoglucosenone. 3-Deoxyglycosulose was experimentally identified from the products of cellulose pyrolysis by Kato and Komorita.⁵⁴ One expeditious pathway to rationalize the formation of 3-deoxyglycosulose from glucose is 1,2-dehydration of D-glucose (reaction 55). DFT calculations of Mayes et al.³⁴ confirmed that this is a plausible reaction with an activation energy of 50.5 kcal·mol⁻¹. 1,2-dehydration of D-glucose undergoes further dehydration, removing the C6-hydroxyl group and H7 on C1, and yields dianhydroglucopyranose that leads to the formation of levoglucosenone (pathway 58-59-60).

1,2-Dehydration can occur at the C6/C5 terminus of D-glucose (reaction 63) and results in removing the 6-hydroxyl group in tandem with the proton on C5 to give 6-deoxyglycosulose, which can lead to the formation of small molecules such as glyoxal, acetol, and acetone.

3.1.2.9. Acetone. Acetone was formed predominantly from C6, C5, and C4 of D-glucose.²⁴ Scheme 2 provides pathway 63-64-65-66-67 by which acetone is formed from the last three carbons of D-glucose. 1,2-Dehydration of 6-deoxyglycosulose gives a dianhydro-D-glucose that undergoes ketonization, affording a tricarbonyl derivative. A retro-aldol reaction followed by decarbonylation occurring to the tricarbonyl species leads to the formation of acetone from C6, C5, and C4.

3.1.2.10. Pyruvaldehyde, Glyceraldehyde, Methylglyoxal, and Dihydroxyacetone. The dominant labeling patterns showed that pyruvaldehyde, methylglyoxal, and dihydroxyacetone were derived from contiguous terminal carbons C6/C5/C4 or C3/C2/C1, and glyceraldehyde is invoked as an

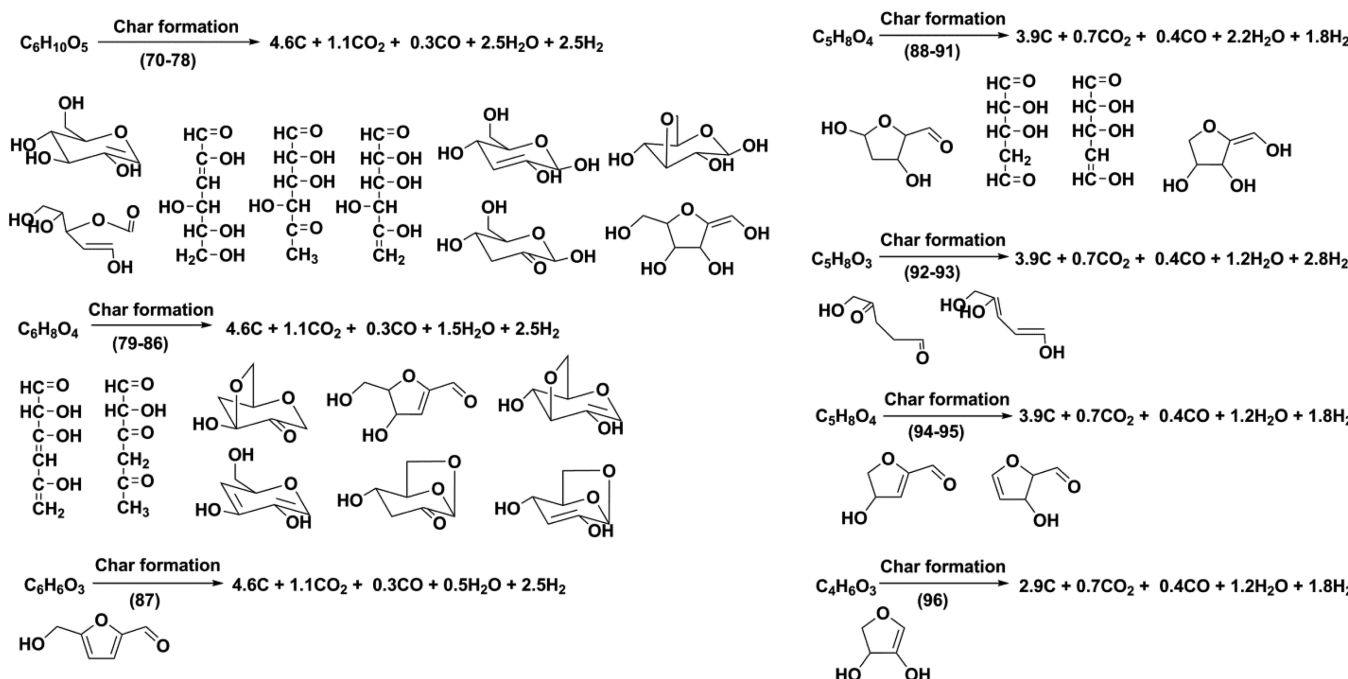
intermediate for the formation of methylglyoxal and 1,3-dihydroxyacetone during fast pyrolysis.²⁴ As shown in Scheme 4, reaction 39 represents a Grob fragmentation on linear D-glucose that yields pyruvaldehyde with C3/C2/C1 and glyceraldehyde from C6/C5/C4. Pathway 40-41-42 depicts the formation of methyl glyoxal from the enol-keto tautomerization of pyruvaldehyde, which can also be formed from intermediate glyceraldehyde via isomerization, followed by dehydration. Glyceraldehyde can isomerize to thermodynamically stable dihydroxyacetone (pathway 40-43).⁵⁵

3.1.2.11. Acetaldehyde. Paine et al.²² revealed that 95% of the acetaldehyde is formed by unimolecular chemistry, and most of it comes from C5/C6. Reaction 7 represents the formation of acetaldehyde through keto–enol tautomerization of ethanol, which formed by retro-aldol of a C4 fragment, involving the coformation of glyoxal.

3.1.2.12. Formaldehyde. The isotopic ¹⁴C-labeling study of Houminer and Hoz⁵⁶ found that the most important source of formaldehyde from glucose is C6, accounting for about 65%, and C1 contributed 15%. Similarly, isotopic labeling with ¹³C by Paine et al.²³ revealed that 70% of the total formaldehyde formed arose from C6 and 17% from C1. Our model included three pathways for the formation of formaldehyde that were proposed by Paine et al.²³ based on their isotopic labeling results. Reaction 25 represents the formation of formaldehyde from C6 via the intermediate D-fructose and the simultaneous coformation of furfural through C–C bond rupture of 5-HMF. Reaction 30 represents the cyclic Grob fragmentation of β -3-ketohexose to afford formaldehyde from C1, water, and a ketene species. The third pathway through reaction 33 represents formaldehyde derived from C6 of D-glucose via Grob fragmentation involving the hydrogen bonding of the C6 hydroxyl-hydrogen to the C4 hydroxyl group.

3.1.2.13. Char Formation. Formation of char is a complicated process and usually involves dehydration and bimolecular condensation reactions of the volatile and condensed phase species. Nimlos et al.³¹ suggested that the dehydration of carbohydrates during biomass fast pyrolysis leads to greater unsaturation and thus cross-linking and then the formation of char, containing about 90% polycyclic aromatic carbons. Brown and co-workers⁵⁷ carried out the characterization of char formed from fast pyrolysis and revealed that char was of high aromaticity. Aromatic clusters typically had 7–8 rings terminated by carbonyl, hydroxyl, or ether groups, and the molecular structure significantly varied with the reaction temperature. The formation of char is also associated with the formation of light gases like CO, CO₂ and H₂, and the existing lumped models track char formation by a single-step, unimolecular reaction that produces char (tracked as carbon, C), CO₂, CO, and H₂ in stoichiometric proportions.^{40,58,59} On the basis of the fact that fast pyrolysis of long-chain cellulose produces much less char compared to glucose, Dauenhauer and co-workers⁷ speculated that the only possible formation route for glucose-derived char is the repolymerization of small molecule species, while cellulosic char can be produced from either repolymerization of volatiles or dehydration without depolymerization. Char formation during cellulose pyrolysis is characterized as involving dehydration.⁶⁰ In this model, because of the lack of understanding of how char structures and compositions vary with reaction conditions at the mechanistic level, char is assumed to be pure carbon, and all the dehydrated species derived from C4–C6 sugars are allowed to form char and light gases, shown as reactions 70–96 in Scheme 5.

Scheme 5. Char Formation of Various Dehydrated Species



We acknowledge that char formation is not fully mechanistic in this work and the above reactions are not the only reactions that might be occurring in cellulose pyrolysis. It is important to keep in mind that pyrolysis is a complex reaction system, and many minor products are still not able to be identified and quantified in experiments and therefore are not included in the model. If new understanding at the mechanistic level emerges from isotopic labeling, electron paramagnetic resonance experiments, and DFT calculations, it is possible to incorporate more detail in our mechanistic model. Another feature of the mechanistic model is that its reaction mechanism can be applied to describe fast pyrolysis of glucose-based carbohydrates. Table 3 presents the number of species and reactions

Table 3. Size of Fast Pyrolysis Model in Terms of the Number of Species and Reactions for Cellulose, Maltohexaose, Cellobiose, and Glucose

carbohydrate	no. of species	no. of reactions
glucose	67	96
cellobiose	79	137
maltohexaose	103	342
cellulose	103	342

involved in the fast pyrolysis models of cellulose, maltohexaose, cellobiose, and glucose, which are all simple derivatives of the full cellulose model. As a demonstration of how these mechanisms extend to form products from fast pyrolysis of glucose-based oligomers and polymers, the reactions in Schemes 1 and 2 are applied to cellobiose, consisting of two glucose molecules linked by a β -(1-4) glycosidic bond, resulting in a set of reactions that can be concisely but fully conveyed, as shown in Scheme S1 in the Supporting Information.

4. SPECIFICATION OF RATE PARAMETERS OF ELEMENTARY REACTIONS

Specification of reasonable values of the rate parameters of the elementary steps in terms of the Arrhenius parameters, activation energy (E_a), and frequency factor (A) is vital for the development of a kinetic model at the mechanistic level. Table 4 contains the rate parameters for reactions included in the mechanistic model, with individual pre-exponential factors, activation energy barriers, and corresponding reference sources for A and E_a . These rate parameters were based on (i) experimentally determined values from the literature, (ii) theoretically estimated values using quantum chemical calculations as reported in the literature, or (iii) fitted values to match the product yields over a wide range of reaction conditions. It should be pointed out, however, that A and E_a values estimated using quantum chemical calculations have uncertainties. For example, the mean unsigned error associated with the B3LYP hybrid functional for activation barriers has been shown to be 4.8 kcal·mol⁻¹.⁶⁵ As compared to our first model,¹⁸ an improvement made by this work is that the model no longer requires a temperature exponent factor (T^n) to capture the temperature dependence of product yields.

The primary goal of the model is to predict the product yields from fast pyrolysis of different glucose-based carbohydrates including glucose, cellobiose, maltohexaose, and cellulose. The reactions of glucose, cellobiose, and other oligomers form a subset of the reactions of cellulose. Therefore, a single set of rate parameters should be applicable to all the reactions irrespective of the initial reactant, if chain length effects are not significant. However, we did include the possibility that the rate of depropagation and end-chain initiation reactions depended on the chain length of the carbohydrate. As shown in Table 4, a smaller value was assigned for A in the depropagation and end-chain initiation of maltohexaose and cellobiose compared to that for cellulose.

The E_a values of all the concerted chain reactions that involve glycosidic bond cleavage are based on the DFT calculations of

Table 4. Arrhenius Rate Parameters of Different Reaction Types Used in Fast Pyrolysis of Glucose-Based Carbohydrates

reaction type	reaction index ^a	A (s^{-1} or $M^{-1}\cdot s^{-1}$)	E_a ^b (kcal·mol ⁻¹)	ref. A	ref. E_a
hydrolysis ^c	IV, vii	1.00×10^{14}	34.0	63	63
initiation	I, ii, v	5.50×10^{14}	53.5	29	29
end-chain-initiation	III, IX, XI, XIII, XIV	5.50×10^{14}	53.5	29	29
	vi	4.00×10^{14}	56.0	36	36
for cellulose	II	3.00×10^{15}	51.5	29	29
for maltohexaose/cellobiose	II	1.30×10^{15}	51.5	29	29
depropagation	VIII	2.00×10^{15}	51.5	29	29
for maltohexaose/cellobiose	VIII	5.00×10^{14}	51.5	29	29
retro-Diels–Alder	VII, XII, ix, 5, 9, 61	1.07×10^{15}	55.0	55	55
dehydration	V, 1	7.00×10^{12}	48.2	34	34
	VI, i, iv, viii, 4	5.00×10^{15}	60.0	fit	34
	X, 8	2.00×10^{15}	54.0	fit	34
	14	5.00×10^{14}	50.0	34	34
	22	1.50×10^{15}	49.7	34	34
	23, 31, 37, 52	7.75×10^{12}	38.9	34	34
	24	5.00×10^{15}	56.5	34	34
	32, 38	5.00×10^{15}	57.5	34	34
	41	1.00×10^9	29.0	32	32
	45	1.00×10^9	27.6	32	32
	53	5.00×10^{15}	61.0	34	34
	55, 63, 64	2.00×10^{15}	50.5	34	34
	58	3.00×10^{13}	47.6	36	36
	60	5.00×10^{12}	47.6	36	36
ring-opening/closing	2	3.90×10^{13}	47.0	34	34
	3	8.30×10^{10}	34.0	34	34
	12	7.50×10^{10}	32.7	34	34
	13	4.30×10^{13}	42.0	34	34
	20	6.00×10^{11}	37.6	34	34
	21	1.60×10^{13}	42.1	34	34
	28	6.65×10^{11}	31.7	35	35
	29	6.65×10^{14}	41.7	35	35
	35, 50	1.28×10^{12}	37.6	34	34
	36, 51	3.37×10^{13}	42.1	34	34
	56	2.15×10^{13}	42.0	34	34
	57	9.44×10^{13}	46.0	34	34
retro-aldo	6, 62	5.64×10^{12}	39.2	35	35
	16	2.29×10^{12}	36.5	35	35
	18	3.74×10^{12}	32.4	35	35
	44, 66, 69	1.00×10^{12}	39.7	35	35
	48	1.00×10^{12}	39.2	35	35
enol-keto tautomerization	10, 17, 34, 54, 59, 65, 68	2.38×10^{13}	46.8	34	34
	7, 42, 43, 46, 49	5.00×10^{15}	57.0	35	35
isomerization	11, 27, 40	2.38×10^{13}	46.8	34	34
	19	4.30×10^{10}	33.4	34	34
cyclic/Grob fragmentation	15, 30	8.00×10^{14}	52.5	32	32
	33, 39	1.50×10^{15}	52.5	32	32
decarbonylation	25, 26, 47, 67	5.00×10^{15}	62.0	fit	64
char formation ^c	70–96	6.50×10^{10}	40.0	58	58

^aReaction indices refer to specific reactions in Schemes 1–4. ^bActivation energies are based on quantum chemical calculations, unless otherwise mentioned. ^c A and E_a are experimentally determined.

Mayes and Broadbelt.²⁹ These values are in line with the reaction barrier of 52 ± 1 kcal·mol⁻¹ for the GBC of methyl β -D-glucoside reported by Hosoya et al.⁶¹ A higher E_a of 56 kcal·mol⁻¹ was used for the end-chain initiation resulting in the formation of 1,2-anhydro-glucopyranose from the chains based on the DFT calculations of Assary and Curtiss,³⁶ in which E_a for GBC of cellobiose to 1,2-dehydro-glucopyranose and β -D-glucopyranose is 59 ± 3 kcal·mol⁻¹.

In our first model, an E_a of 51.5 kcal·mol⁻¹ and A of 2×10^{15} s⁻¹ were applied for the entire family of 1,2- and 1,3-dehydration reactions of the glucose molecules.¹⁸ Recently, Mayes et al.³⁴ found that 1,2-dehydration of β -D-glucopyranose to cyclic enols has high energy barriers, mostly over 70 kcal·mol⁻¹, which means those 1,2-dehydration reactions are very slow even with an artificially inflated unimolecular A of 10^{16} s⁻¹. These findings are also consistent with a reported E_a of 65 ± 2 kcal·mol⁻¹ for 1,2-dehydration reactions of the pyranose ring

involving a cyclic, four-membered transition state. The model here included only the most feasible 1,2-dehydration of β -D-glucopyranose (reaction 4), requiring an E_a of 62 kcal·mol⁻¹ to give 1,2-anhydro-glucopyranose according to the DFT calculations of Mayes et al.,³⁴ and E_a was adjusted to be 60 kcal·mol⁻¹ within the limits of uncertainty to match the experimental data. However, 1,2-dehydration of glucose in its acyclic form (reaction 55) requires a much lower activation energy, 50.5 kcal·mol⁻¹. Lower barriers are also involved in the dehydration to a furan ring (reactions 22, 23, and 24).

For other dehydration reactions, most of the kinetic parameters, especially E_a , are applied here without adjustment from the literature. For example, the model utilized an E_a of 48.2 kcal·mol⁻¹ and A of 7.0×10^{12} s⁻¹ for the one-step dehydration of β -D-glucopyranose to 1,6-anhydro-glucopyranose (reaction 1), for which E_a of 48.2 kcal·mol⁻¹ and A of 1.4×10^{13} s⁻¹ were reported by Mayes et al.³⁴ The same kinetic parameters are also applied to similar dehydration reactions occurring to the end-groups of carbohydrate chains (reactions 1 and V, and reactions 4, VI and viii). However, dehydration reactions occurring at the mid-groups of the chains are expected to possess a higher E_a because of the decreased flexibility of the chains and intramolecular hydrogen bonding. Therefore, a higher activation energy of 60 kcal·mol⁻¹ is used here for the formation of 3,6-anhydroglucopyranose residues via midchain dehydration (reactions i and iv), as compared to E_a of 54 kcal·mol⁻¹ for dehydration reactions X and 8 resulting in 3,6-anhydro-glucose formation. Dehydration of glucose with the involvement of losing HO6 and the hydroxyl group at C1–C4 to form water and anhydro-glucose is more feasible and thus has a lower energy barrier than that requiring the involvement of the hydroxyl group at C1–C4 and H at its adjacent C. For example, E_a for dehydration to levoglucosan is 48 kcal·mol⁻¹ versus E_a of 60 kcal·mol⁻¹ for 1,2-dehydration of glucose to 1,2-anhydro-glucopyranose. E_a of dehydration of β -D-glucofuranose to anhydro- β -D-glucofuranose reported by Mayes et al.³⁴ has been applied here without adjustment. A similar activation energy of 49.3 kcal·mol⁻¹ was reported by Seshadri and Westmoreland.³⁵ Kinetic parameters for the dehydration of β -D-fructose to 5-HMF have been applied to similar dehydration reactions resulting in the formation of other furans such as furfural and furanone. E_a and A of the dehydration (reactions 58 and 60) that results in the formation of levoglucosenone are from quantum chemical calculations of Assary and Curtiss.³⁶ E_a and A for the dehydration of small molecules (reactions 41 and 45) are based on DFT calculations of Shen et al.³²

The kinetic parameters for various retro-aldol reactions are based on the work of Seshadri and Westmoreland,³⁵ who reported concerted transition states, reaction pathways based on elementary steps, and rate coefficients for the pyrolysis of β -D-glucose. They revealed that retro-aldol condensation is a favorable unimolecular reaction in glucose pyrolysis because of its low activation energy ranging from 30 to 40 kcal·mol⁻¹. The kinetic parameters are also consistent with the values reported by Assary and Curtiss⁵⁵ who carried out high-level quantum chemical calculations (Gaussian-4 (G4) theory) to unravel the reactions of glucose and fructose.

The kinetic parameters for isomerization and tautomerization reactions are based on quantum chemical calculations of Seshadri and Westmoreland³⁵ and Mayes et al.³⁴ A set of E_a and A values from quantum chemical calculations of Carstensen and Dean⁴² is applied for all the retro-Diels–Alder reactions in the

model. A similar activation energy of 54.5 kcal·mol⁻¹ for retro-Diels–Alder of glucose was also reported by Shen et al.,³² who also reported an energy barrier of 52 ± 2 kcal mol⁻¹ for the Grob fragmentation reaction of acyclic glucose. The model used 52.5 kcal·mol⁻¹ for E_a for all the cyclic/Grob fragmentations of D-glucose and its isomers with ring structures, while A values were adjusted within the limits of uncertainty to address the difference between cyclic and Grob fragmentations.

The conversion between β -D-glucopyranose and its isomers proceeds via ring-opening and ring-closing as well as isomerization reactions. The previous model used E_a of 59 kcal·mol⁻¹ and a temperature exponent of 1.5 for all the ring-opening reactions because of the lack of kinetic parameters available at the time the model was created.¹⁸ As is clear from Table 4, a much lower E_a was used for ring-opening reactions in this model. These kinetic parameters are based on quantum chemical calculations of Mayes et al.³⁴ and Seshadri and Westmoreland,³⁵ mostly applied here without adjustment.

Zhang et al.⁶² reported that the activation energies of decarbonylation during fast pyrolysis range from 57.5 to 67.1 kcal·mol⁻¹. We used an E_a of 62 kcal·mol⁻¹ for the decarbonylation of 5-HMF to furanmethanol and assigned the same value for E_a of other decarbonylation reactions and C–C bond rupture on the other substituent of 5-HMF to form furfural. For thermohydrolysis and char formation, the rate parameters estimated through experiments⁵⁸ were utilized. It should be pointed out that the same A and E_a values for a particular reaction family were used in the model to reduce the number of parameters that were fit. The majority of the E_a and A values are obtained from previously published reports, while a few frequency factors have been fitted to capture the product yields.

5. SUMMARY

In this work, the product distribution arising from the fast pyrolysis of neat glucose-based carbohydrates, including glucose, cellobiose, maltohexaose, and cellulose, was studied using a micropyrolyzer system. A total of 32 pyrolysis products were identified, and their quantified yields were reported. We developed an enhanced mechanistic model for fast pyrolysis of neat glucose-based carbohydrates by integrating currently known reactions and pathways, especially the newly discovered concerted mechanisms for the formation of various pyrolysis products and the associated kinetic parameters of elementary reactions as well as experimental findings. The model tracks 103 species consisting of a wide range of cellulosic chains and LMWPs in 342 individual reactions, which includes decomposition reactions of cellulosic chains via initiation, depropagation, end-chain initiation, thermohydrolysis, dehydration, 1,2-dehydration, midchain dehydration, and retro-Diels–Alder reactions, and the formation of 67 LMWPs via ring opening/closing, dehydration, 1,2-dehydartion, isomerization, retro-aldol, retro-Diels–Alder, cyclic/Grob fragmentation, and enol-keto tautomerization. The experimental data will be used to validate the mechanistic model in the second part of this study (DOI 10.1021/ie502260q).

ASSOCIATED CONTENT

Supporting Information

Standard deviation of the yields of products (in weight percent) from fast pyrolysis of cellulose at different temperatures (Table S1) and glucose, cellobiose, and maltohexaose at 500 °C (Table S2); molecular structure, atom type, and numbering scheme of

β -D-glucopyranose (Figure S1); and mechanism of cellobiose degradation during fast pyrolysis (Scheme S1). This material is available free of charge via the Internet at <http://pubs.acs.org>.

AUTHOR INFORMATION

Corresponding Authors

*E-mail: bshanks@iastate.edu. Tel: +1-515-294-1895.

*E-mail: broadbelt@northwestern.edu. Fax: +1-847-491-3728. Tel: +1-847-491-5351.

Notes

The authors declare no competing financial interest.

ACKNOWLEDGMENTS

The authors are grateful for financial support provided by the Department of Energy (DOE) Office of Energy Efficiency and Renewable Energy (EERE) through the Office of Biomass Program, Grant DEEE0003044. The authors thank Dr. R. Vinu and Abraham J. Yanez-McKay for fruitful discussions and useful suggestions.

REFERENCES

- (1) Hildebrandt, D.; Glasser, D.; Hausberger, B.; Patel, B.; Glasser, B. J. Producing Transportation Fuels with Less Work. *Science* **2009**, *323*, 1680–1681.
- (2) Miller, I. J.; Fellows, S. K. Liquefaction of Biomass as a Source of Fuels or Chemicals. *Nature (London, U.K.)* **1981**, *289*, 398–399.
- (3) Kunke, E. L.; Simonetti, D. A.; West, R. M.; Serrano-Ruiz, J. C.; Gärtner, C. A.; Dumescic, J. A. Catalytic Conversion of Biomass to Monofunctional Hydrocarbons and Targeted Liquid-Fuel Classes. *Science* **2008**, *322*, 417–421.
- (4) Regalbuto, J. R. Cellulosic Biofuels—Got Gasoline? *Science* **2009**, *325*, 822–824.
- (5) Vispute, T. P.; Zhang, H.; Sanna, A.; Xiao, R.; Huber, G. W. Renewable Chemical Commodity Feedstocks from Integrated Catalytic Processing of Pyrolysis Oils. *Science* **2010**, *330*, 1222–1227.
- (6) Paulsen, A. D.; Mettler, M. S.; Dauenhauer, P. J. The Role of Sample Dimension and Temperature in Cellulose Pyrolysis. *Energy Fuels* **2013**, *27*, 2126–2134.
- (7) Mettler, M. S.; Vlachos, D. G.; Dauenhauer, P. J. Top Ten Fundamental Challenges of Biomass Pyrolysis for Biofuels. *Energy Environ. Sci.* **2012**, *5*, 7797–7809.
- (8) Bridgwater, A. V. Review of Fast Pyrolysis of Biomass and Product Upgrading. *Biomass Bioenergy* **2012**, *38*, 68–94.
- (9) Butler, E.; Devlin, G.; Meier, D.; McDonnell, K. A Review of Recent Laboratory Research and Commercial Developments in Fast Pyrolysis and Upgrading. *Renewable Sustainable Energy Rev.* **2011**, *15*, 4171–4186.
- (10) Mohan, D.; Pittman, C. U.; Steele, P. H. Pyrolysis of Wood/Biomass for Bio-oil: A Critical Review. *Energy Fuels* **2006**, *20*, 848–889.
- (11) Bridgwater, A. V.; Meier, D.; Radlein, D. An Overview of Fast Pyrolysis of Biomass. *Org. Geochem.* **1999**, *30*, 1479–1493.
- (12) Várhegyi, G.; Antal, M. J., Jr.; Jakab, E.; Szabó, P. Kinetic Modeling of Biomass Pyrolysis. *J. Anal. Appl. Pyrolysis* **1997**, *42*, 73–87.
- (13) Lédé, J. Cellulose Pyrolysis Kinetics: An Historical Review on the Existence and Role of Intermediate Active Cellulose. *J. Anal. Appl. Pyrolysis* **2012**, *94*, 17–32.
- (14) Bradbury, A. G. W.; Sakai, Y.; Shafizadeh, F. Kinetic-Model for Pyrolysis of Cellulose. *J. Appl. Polym. Sci.* **1979**, *23*, 3271–3280.
- (15) White, J. E.; Catallo, W. J.; Legendre, B. L. Biomass Pyrolysis Kinetics: A Comparative Critical Review with Relevant Agricultural Residue Case Studies. *J. Anal. Appl. Pyrolysis* **2011**, *91*, 1–33.
- (16) Ţerbănescu, C. Kinetic Analysis of Cellulose Pyrolysis: A Short Review. *Chem. Pap.* **2014**, *68*, 1–14.
- (17) Lin, T.; Goos, E.; Riedel, U. A Sectional Approach for Biomass: Modelling the Pyrolysis of Cellulose. *Fuel Process. Technol.* **2013**, *115*, 246–253.
- (18) Vinu, R.; Broadbelt, L. J. A Mechanistic Model of Fast Pyrolysis of Glucose-Based Carbohydrates to Predict Bio-oil Composition. *Energy Environ. Sci.* **2012**, *5*, 9808–9826.
- (19) Patwardhan, P. R.; Satrio, J. A.; Brown, R. C.; Shanks, B. H. Product Distribution from Fast Pyrolysis of Glucose-Based Carbohydrates. *J. Anal. Appl. Pyrolysis* **2009**, *86*, 323–330.
- (20) Patwardhan, P. R.; Satrio, J. A.; Brown, R. C.; Shanks, B. H. Influence of Inorganic Salts on the Primary Pyrolysis Products of Cellulose. *Bioresour. Technol.* **2010**, *101*, 4646–4655.
- (21) Patwardhan, P. R.; Dalluge, D. L.; Shanks, B. H.; Brown, R. C. Distinguishing Primary and Secondary Reactions of Cellulose Pyrolysis. *Bioresour. Technol.* **2011**, *102*, 5265–5269.
- (22) Paine, J. B., III; Pithawalla, Y. B.; Naworal, J. D.; Thomas, C. E. Carbohydrate Pyrolysis Mechanisms from Isotopic Labeling: Part 1: The Pyrolysis of Glycerin: Discovery of Competing Fragmentation Mechanisms Affording Acetaldehyde and Formaldehyde and the Implications for Carbohydrate Pyrolysis. *J. Anal. Appl. Pyrolysis* **2007**, *80*, 297–311.
- (23) Paine, J. B., III; Pithawalla, Y. B.; Naworal, J. D. Carbohydrate Pyrolysis Mechanisms from Isotopic Labeling: Part 2. The Pyrolysis of D-Glucose: General Disconnetive Analysis and The Formation of C1 and C2 Carbonyl Compounds by Electrocyclic Fragmentation Mechanisms. *J. Anal. Appl. Pyrolysis* **2008**, *82*, 10–41.
- (24) Paine, J. B., III; Pithawalla, Y. B.; Naworal, J. D. Carbohydrate Pyrolysis Mechanisms from Isotopic Labeling: Part 3. The Pyrolysis of D-Glucose: Formation of C3 and C4 Carbonyl Compounds and a Cyclopentenedione Isomer by Electrocyclic Fragmentation Mechanisms. *J. Anal. Appl. Pyrolysis* **2008**, *82*, 42–69.
- (25) Paine, J. B., III; Pithawalla, Y. B.; Naworal, J. D. Carbohydrate Pyrolysis Mechanisms from Isotopic Labeling: Part 4. The Pyrolysis of D-Glucose: The Formation of Furans. *J. Anal. Appl. Pyrolysis* **2008**, *83*, 37–63.
- (26) Richards, G. N. Glycolaldehyde from Pyrolysis of Cellulose. *J. Anal. Appl. Pyrolysis* **1987**, *10*, 251–255.
- (27) Ponder, G. R.; Richards, G. N.; Stevenson, T. T. Influence of Linkage Position and Orientation in Pyrolysis of Polysaccharides: A Study of Several Glucans. *J. Anal. Appl. Pyrolysis* **1992**, *22*, 217–229.
- (28) Ponder, G. R.; Richards, G. N. Pyrolysis of Some ^{13}C -Labeled Glucans: A Mechanistic Study. *Carbohydr. Res.* **1993**, *244*, 27–47.
- (29) Mayes, H. B.; Broadbelt, L. J. Unraveling the Reactions that Unravel Cellulose. *J. Phys. Chem. A* **2012**, *116*, 7098–7106.
- (30) Hosoya, T.; Sakaki, S. Levoglucosan Formation from Crystalline Cellulose: Importance of a Hydrogen Bonding Network in the Reaction. *ChemSusChem* **2013**, *6*, 2356–2368.
- (31) Nimlos, M. R.; Blanksby, S. J.; Ellison, G. B.; Evans, R. J. Enhancement of 1,2-Dehydration of Alcohols by Alkali Cations and Protons: A Model for Dehydration of Carbohydrates. *J. Anal. Appl. Pyrolysis* **2003**, *66*, 3–27.
- (32) Shen, C.; Zhang, I. Y.; Fu, G.; Xu, X. Pyrolysis of D-Glucose to Acrolein. *Chin. J. Chem. Phys.* **2011**, *24*, 249–252.
- (33) Vinu, R.; Broadbelt, L. J. Unraveling Reaction Pathways and Specifying Reaction Kinetics for Complex Systems. *Annu. Rev. Chem. Biomol. Eng.* **2012**, *3*, 29–54.
- (34) Mayes, H. B.; Nolte, M. W.; Beckham, G. T.; Shanks, B. H.; Broadbelt, L. J. The Alpha-Beta(α) of Glucose Pyrolysis: Computational and Experimental Investigations of 5-Hydroxymethylfurfural and Levoglucosan Formation Reveal Implications for Cellulose Pyrolysis. *ACS Sustainable Chem. Eng.* **2014**, *2*, 1461–1473.
- (35) Seshadri, V.; Westmoreland, P. R. Concerted Reactions and Mechanism of Glucose Pyrolysis and Implications for Cellulose Kinetics. *J. Phys. Chem. A* **2012**, *116*, 11997–12013.
- (36) Assary, R. S.; Curtiss, L. A. Thermochemistry and Reaction Barriers for the Formation of Levoglucosanone from Cellobiose. *ChemCatChem* **2012**, *4*, 200–205.
- (37) Vasiliou, A. K.; Kim, J. H.; Ormond, T. K.; Piech, K. M.; Urness, K. N.; Scheer, A. M.; Robichaud, D. J.; Mukarakate, C.; Nimlos, M. R.;

- Daily, J. W.; Guan, Q.; Carstensen, H. H.; Ellison, G. B. Biomass Pyrolysis: Thermal Decomposition Mechanisms of Furfural and Benzaldehyde. *J. Chem. Phys.* **2013**, *139*, 4310.
- (38) Agarwal, V.; Dauenhauer, P. J.; Huber, G. W.; Auerbach, S. M. Ab Initio Dynamics of Cellulose Pyrolysis: Nascent Decomposition Pathways at 327 and 600 °C. *J. Am. Chem. Soc.* **2012**, *134*, 14958–14972.
- (39) Norinaga, K.; Shoji, T.; Kudo, S.; Hayashi, J. Detailed Chemical Kinetic Modelling of Vapour-Phase Cracking of Multi-component Molecular Mixtures Derived from the Fast Pyrolysis of Cellulose. *Fuel* **2013**, *103*, 141–150.
- (40) Lin, Y. C.; Cho, J.; Tompsett, G. A.; Westmoreland, P. R.; Huber, G. W. Kinetics and Mechanism of Cellulose Pyrolysis. *J. Phys. Chem. C* **2009**, *113*, 20097–20107.
- (41) Mettler, M. S.; Paulsen, A. D.; Vlachos, D. G.; Dauenhauer, P. J. Pyrolytic Conversion of Cellulose to Fuels: Levoglucosan Deoxygenation via Elimination and Cyclization within Molten Biomass. *Energy Environ. Sci.* **2012**, *5*, 7864–7868.
- (42) Hans-Heinrich, C.; Anthony, M. D. Development of Detailed Kinetic Models for the Thermal Conversion of Biomass via First Principle Methods and Rate Estimation Rules. In *Computational Modeling in Lignocellulosic Biofuel Production*; Nimlos, M. R., Crowley, M. F., Eds.; ACS Symposium Series; American Chemical Society: Washington, DC, 2010; Vol. 1052, pp 201–243.
- (43) Shen, D. K.; Gu, S. The Mechanism for Thermal Decomposition of Cellulose and Its Main Products. *Bioresour. Technol.* **2009**, *100*, 6496–6504.
- (44) Slamet, R.; Wege, D. Preparation of Isobenzofurandiones by Flash Vacuum Pyrolysis Involving Retro-Diels–Alder Expulsion of Ethylene and Concomitant C–O Cleavage of Methoxy or Ethyl-enedioxy Groups. *Tetrahedron* **2007**, *63*, 12621–12628.
- (45) Kawamoto, H.; Murayama, M.; Saka, S. Pyrolysis Behavior of Levoglucosan as an Intermediate in Cellulose Pyrolysis: Polymerization into Polysaccharide as a Key Reaction to Carbonized Product Formation. *J. Wood Sci.* **2003**, *49*, 469–473.
- (46) Bahng, M. K.; Carstensen, H. H.; Vasiliou, A.; Ellison, G. B.; Nimlos, M. R. Thermal Degradation Pathways of Levoglucosan as an Intermediate in Cellulose Pyrolysis. *Abstr. Pap. Am. Chem. Soc.* **2009**, *237*.
- (47) Shafizadeh, F.; Fu, Y. L. Pyrolysis of Cellulose. *Carbohydr. Res.* **1973**, *29*, 113–122.
- (48) Mettler, M. S.; Mushrif, S. H.; Paulsen, A. D.; Javadekar, A. D.; Vlachos, D. G.; Dauenhauer, P. J. Revealing Pyrolysis Chemistry for Biofuels Production: Conversion of Cellulose to Furans and Small Oxygenates. *Energy Environ. Sci.* **2012**, *5*, 5414–5424.
- (49) Sanders, E. B.; Goldsmith, A. I.; Seeman, J. I. A Model that Distinguishes the Pyrolysis of D-Glucose, D-Fructose, and Sucrose from that of Cellulose. Application to the Understanding of Cigarette Smoke Formation. *J. Anal. Appl. Pyrolysis* **2003**, *66*, 29–50.
- (50) Lin, X. F.; Qu, Y. Y.; Lv, Y. H.; Xi, Y. Y.; Phillips, D. L.; Liu, C. G. The First Dehydration and the Competing Reaction Pathways of Glucose Homogeneously and Heterogeneously Catalyzed by Acids. *Phys. Chem. Chem. Phys.* **2013**, *15*, 2967–2982.
- (51) Fabbri, D.; Torri, C.; Mancini, I. Pyrolysis of Cellulose Catalysed by Nanopowder Metal Oxides: Production and Characterisation of a Chiral Hydroxylactone and Its Role as Building Block. *Green Chem.* **2007**, *9*, 1374–1379.
- (52) Meier, D.; Fortmann, I.; Odermatt, J.; Faix, O. Discrimination of Genetically Modified Poplar Clones by Analytical Pyrolysis–Gas Chromatography and Principal Component Analysis. *J. Anal. Appl. Pyrolysis* **2005**, *74*, 129–137.
- (53) Pattiya, A.; Titiloye, J. O.; Bridgwater, A. V. Fast Pyrolysis of Cassava Rhizome in the Presence of Catalysts. *J. Anal. Appl. Pyrolysis* **2008**, *81*, 72–79.
- (54) Kato, K.; Komorita, H. Pyrolysis of Cellulose. Part V. Isolation and Identification of 3-Deoxyglycosones Produced from D-Glucose, D-Xylose and α-Cellulose by Heating. *Agric. Biol. Chem.* **1968**, *32*, 715–720.
- (55) Assary, R. S.; Curtiss, L. A. Comparison of Sugar Molecule Decomposition through Glucose and Fructose: A High-level Quantum Chemical Study. *Energy Fuels* **2012**, *26*, 1344–1352.
- (56) Houminer, Y.; Hoz, S. Formation of Formaldehyde in the Thermal Decomposition of D-Glucose Labelled with ¹⁴C at Various Positions. *Isr. J. Chem.* **1970**, *8*, 97–98.
- (57) Brewer, C. E.; Schmidt-Rohr, K.; Satrio, J. A.; Brown, R. C. Characterization of Biochar from Fast Pyrolysis and Gasification Systems. *Environ. Prog. Sustainable Energy* **2009**, *28*, 386–396.
- (58) Cho, J. M.; Davis, J. M.; Huber, G. W. The Intrinsic Kinetics and Heats of Reactions for Cellulose Pyrolysis and Char Formation. *ChemSusChem* **2010**, *3*, 1162–1165.
- (59) Ranzi, E.; Cuoci, A.; Faravelli, T.; Frassoldati, A.; Migliavacca, G.; Pierucci, S.; Sommariva, S. Chemical Kinetics of Biomass Pyrolysis. *Energy Fuels* **2008**, *22*, 4292–4300.
- (60) Milosavljevic, I.; Oja, V.; Suuberg, E. M. Thermal Effects in Cellulose Pyrolysis: Relationship to Char Formation Processes. *Ind. Eng. Chem. Res.* **1996**, *35*, 653–662.
- (61) Hosoya, T.; Nakao, Y.; Sato, H.; Kawamoto, H.; Sakaki, S. Thermal Degradation of Methyl β-D-Glucoside. A Theoretical Study of Plausible Reaction Mechanisms. *J. Org. Chem.* **2009**, *74*, 6891–6894.
- (62) Zhang, X. L.; Yang, W. H.; Blasiak, W. Kinetics Study on Thermal Dissociation of Levoglucosan during Cellulose Pyrolysis. *Fuel* **2013**, *109*, 476–483.
- (63) Pilath, H. M.; Nimlos, M. R.; Mittal, A.; Himmel, M. E.; Johnson, D. K. Glucose Reversion Reaction Kinetics. *J. Agric. Food Chem.* **2010**, *58*, 6131–6140.
- (64) Huang, J.; Liu, C.; Wei, S.; Huang, X.; Li, H. Density Functional Theory Studies on Pyrolysis Mechanism of β-D-Glucopyranose. *J. Mol. Struct.: THEOCHEM* **2010**, *958*, 64–70.
- (65) Lynch, B. J.; Fast, P. L.; Harris, M.; Truhlar, D. G. Adibatic Connection for Kinetics. *J. Phys. Chem. A* **2000**, *104* (21), 4811–4815.